Evaluation of Single and Dual Image Object Detection through Image Segmentation Using ResNet18 in Robotic Vision Applications

Phichitphon Chotikunnan [1], Tasawan Puttasakul [2*], Rawiphon Chotikunnan [3], Benjamas Panomruttanarug [4],
Manas Sangworasil [5], Anuchart Srisiriwat [6]
[1, 2, 3, 5] College of Biomedical Engineering, Rangsit University, Pathum Thani, Thailand
[4] Department of Control and Instrumentation Engineering, King Mongkut's University of Technology Thonburi, Bangkok, Thailand
[6] Department of Electrical Engineering, Pathumwan Institute of Technology, Bangkok, Thailand
Email: [1] phichitphon.c@rsu.ac.th, [2] tasawan.p@rsu.ac.th, [3] rawiphon.c@rsu.ac.th
[4] benjamas.pan@kmutt.ac.th, [5] manas.s@rsu.ac.th, [6] anuchart@pit.ac.th
*Corresponding Author

Abstract— **This study presents a method for enhancing the accuracy of object detection in industrial automation applications using ResNet18-based image segmentation. The objective is to extract object images from the background image accurately and efficiently. The study includes three experiments, RGB to grayscale conversion, single image processing, and dual image processing. The results of the experiments show that dual image processing is superior to both RGB to grayscale conversion and single image processing techniques in accurately identifying object edges, determining CG values, and cutting background images and gripper heads. The program achieved a 100% success rate for objects located in the workpiece tray, while also identifying the color and shape of the object using ResNet-18. However, single image processing may have advantages in certain scenarios with sufficient image information and favorable lighting conditions. Both methods have limitations, and future research could focus on further improvements and optimization of these methods, including separating objects into boxes of each type and converting image coordinate data into robot working area coordinates. Overall, this study provides valuable insights into the strengths and limitations of different object recognition techniques for industrial automation applications.**

Keywords— Robotic vision; Dual design; Image segmentation; Object Detection; ResNet18.

I. INTRODUCTION

Robotic arms have experienced significant development and widespread adoption across various industries, including automotive, electronics, pharmaceuticals, food processing, and aerospace. These versatile machines have evolved over the years, with advances in computer-controlled electrical systems, sensors, artificial intelligence, and machine vision enhancing their capabilities. Recently, collaborative robots, or cobots, have emerged as a new category designed to work safely alongside humans in shared workspaces. The integration of machine learning and AI has further expanded the applications of robotic arms into fields such as healthcare, where they assist in surgery, and space exploration, where they perform maintenance tasks on the international space station. The continuous advancement of technology promises even greater potential for robotic arms in the future.

Robotic vision technology offers a wide range of applications across various domains, making it a vital component of modern industries. In agriculture, it is employed for tasks such as detecting different fruit types using faster R-CNN systems, estimating fruit quantity and ripeness, evaluating crop harvests, and identifying plant diseases [1]-[9]. Besides agriculture, robotic vision technology is utilized for facial recognition [12]-[18], classroom location, public identity verification, and payment processing [19]. It can also determine if a person is wearing a mask [20]. Moreover, this technology is extensively used for object detection in diverse areas, including survey research, passenger detection in buses, and traffic management applications [21]-[29].

Having been in use for an extended period, this technology incorporates various techniques like CNN or R-CNN, multiscale image blocking, deep learning, and machine learning [23]-[33]. Image segmentation, a critical process in robotic vision technology, involves separating objects within an image by identifying specific points or coordinates of interest [34]-[36]. This technique has multiple applications across different fields, such as topographic surveys [37]-[39], medical research [40]-[43], and plant disease recognition [46], among others.

To achieve accurate image segmentation, multilevel thresholding techniques based on energy curves with harmony search algorithms or CNN techniques [44], as well as deep convolutional neural networks (DCNNs) [45], can be used. Examples of image segmentation applications include pathological image analysis [47], segmentation of lungs in chest X-ray images [48], brain tumor classification [49], COVID-19 diagnosis [50], and crack detection using image processing [51].

Expert systems, a type of artificial intelligence control system, are crucial in many fields, including medicine, engineering, and finance [52]-[54]. They simulate human decision-making processes by using a knowledge base and a set of rules to make decisions, making them valuable in situations requiring accurate and consistent decisions based

on specific criteria. Expert systems are primarily used in diagnosis [55]-[59] and can be combined with other systems, such as fuzzy expert systems [60], [61], fuzzy neural network expert systems [62], and neural network expert systems [63], to enhance their performance and diversity.

Neural networks play a crucial role in processing visual signals, with convolutional neural networks (CNNs) being widely employed in various applications such as dental image diagnostics [64], agriculture [65], and chest disease examination [66]. Residual neural networks, also known as ResNets [76]-[78], are a specific type of artificial neural network used in diverse applications, including image processing and disease detection. Due to their versatility, ResNets are popular across numerous fields and have multiple implementations, such as ResNet-18 [78], [79], ResNet-34 [80], ResNet-50 [81], and ResNet-101 [82]. The integration of these technologies can also extend to the development of multi-robotic arm systems [32] and mobile robots capable of facial detection [33]. This combination has led to the creation of increasingly accurate systems while streamlining the design process through the use of various tools and functions. As a result, these advancements continue to contribute to the ongoing progress of robotic vision technology.

This study focuses on the development and implementation of image preparation techniques for both single and dual image object detection using image segmentation, with potential applications in the realm of robotic vision systems. By leveraging the ResNet18 neural network for object detection based on color and shape, the research explores two image preparation procedures: single image preparation, which uses an expert system to validate the RGB color scale, and dual image preparation, which compares data differences between two images for more accurate object area determination before image segmentation. Additionally, the study calculates the center of gravity (CG) value of the image. The experimental results showcase the effectiveness of these approaches in collaboration with ResNet18 for identifying various object types, emphasizing the significance of this research as a case study in object detection through image segmentation and its potential impact on robotic vision applications.

II. METHOD

A. Robotic Vision

This research presents a robotic vision design, illustrated in Fig. 1 as a block diagram, that employs a collaborative structure between computer and robots. The design includes a computer system equipped with a camera to detect the location of an object, and the location information is then transmitted to the MATLAB program for image processing and object separation. The robot's operating system can be controlled by exchanging data with a computer. The Arduino microcontroller board can operate in real-time by connecting to the MATLAB & Simulink program. While other research studies have proposed various designs for the system, such as micro-robotics [83], Microgrid [84], mini drone [85], DC motor control [86], [87], BLDC motor [88], lane-keeping control [89], and hexapod robot [90], none of them have focused on image processing. Nonetheless, these studies

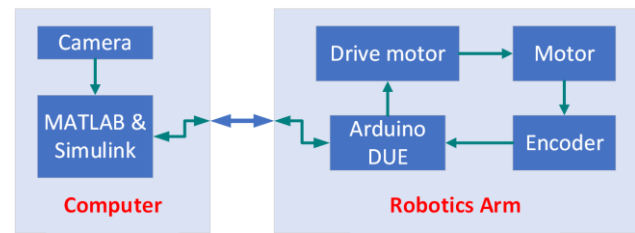illustrate the potential applications of robotic vision design in different areas of robotics.

Fig. 1. Block diagram of the overall system.

This study presents a sample design for the robot's working area, as shown in Fig. 2 and Fig. 3 illustrates the various positioning areas of the robot from a top view, which includes the camera, the robot, the workpiece area, and the workbox. To minimize outside interference, the camera is installed in a closed room, and the room is illuminated with white neon lights. The camera is positioned at a height of 65 cm above the workpiece tray, which measures 28 cm by 18 cm.
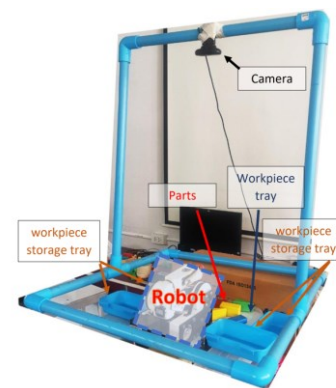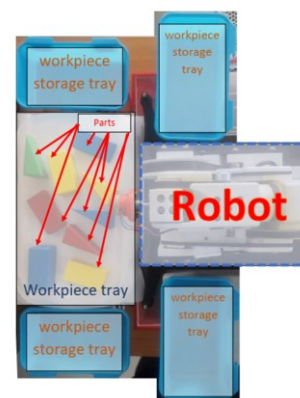

Fig. 2. Overview of the work area.

Fig. 3. Overview of the top view work area.

Fig. 4 shows different robots that are compatible with the robotic vision system. These robots include the mechanical arm robot [91], [92], scala robot, and cartesian robot [93]-[97]. Additionally, industrial motors can be integrated into the robotic vision system. Furthermore, mobile robots can also be applied to the machine vision system [98], [99].
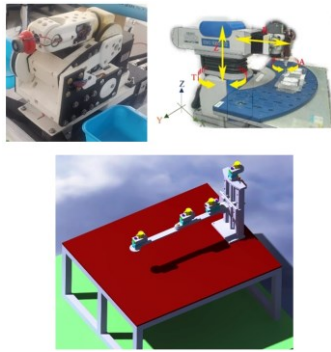
Fig. 4. An example of a robot utilizing robotic vision.

The research design's main objective is to enable the robot to detect objects in the work area and automatically pick them up to place them in a workpiece box. The workpiece box may be divided based on the object's color or shape. The entire system design comprises three parts, as illustrated in Fig. 5, which are explained in detail below:

1. Computer vision, which involves image processing, object coordinate identification, object color separation, and object shape separation.

2. Robot trajectory design.

3. Object retrieval and placement.

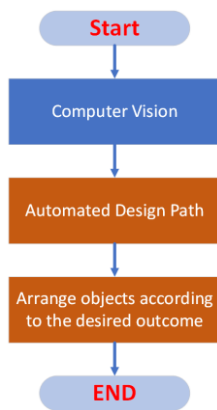However, this research will only present part 1 of the design.

Fig. 5. Diagram of the overall system in the robotic vision procedure.

B. Hardware Implementations

This section describes the components utilized in the image processing phase of this research, including the HD webcam and a notebook ASUS TUF gaming FX506LI-HN091T.

The Logitech HD webcam C170 was chosen as the camera for this research due to its cost-effectiveness. This camera is primarily designed for video calling and offers seamless communication with friends and family through most major instant messengers. Logitech fluid crystal technology enhances the camera's video quality, providing smoother video, sharper pictures, richer colors, and clearer sound in real-world conditions. The camera has a standard

resolution of 640×480 pixels. However, video capture can be set to 1024×768 pixels, and photos can be captured at up to 5 MP. The camera connects via Hi-Speed USB 2.0, as certified by the manufacturer. The camera body is presented in Fig. 6.

Fig. 6. Logitech HD webcam C170.

The second piece of equipment used in this research is the notebook ASUS TUF gaming FX506LI-HN091T, which features an intel core I7-10870H CPU, a GTX 1650TI 4GB GDDR6 video card, a 15.6" Full HD IPS 144Hz adaptive sync display, 16 GB DDR4 2933 MHz RAM, and a 512 GB SSD M.2. This equipment was utilized for image processing operations and controlling the robot through the MATLAB R2022b program, as illustrated in Fig. 7.

Fig. 7. Asus TUF Gaming FX506LI-HN091T.

III. IMAGE PROCESSING AND IMAGE SEGMENTATION

A. Overview of the Image processing Procedure

This section provides an overview of the computer vision system's functionality, which can be separated into internal components as shown in Fig. 8.
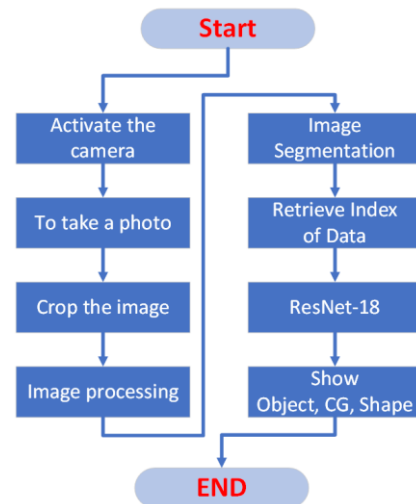

Fig. 8. Program flowchart of image processing.

The system receives data from a camera mounted on top of the robot, as depicted in Fig. 2, and then the computer activates the camera to obtain the different positions of the robot in Fig. 3. When the robot takes pictures or captures images for processing, the program system cuts the image only to the part that will be in focus for image processing.

The image obtained from image processing is then framed and stored in the ResNet-1 8 system to sort the images according to the inspection target and display the results of the running and ending the program.

This section describes the program flowchart for image processing, as depicted in Fig. 8. The first step to activate the camera in MATLAB is to install the MATLAB support package for USB webcams, as shown in Fig. 9. Next, the webcam object is initialized using the command "cam = webcam", and the video stream can be previewed using "preview(cam)" as shown in Fig. 10. To capture an image from the camera, the "snapshot(cam)" command is used to store the image as RGB image data in a program variable.

To reduce the image size and processing time, the image is cropped to select the area of interest in image processing. In this research, the coordinates (252, 323) and (800, 663) are used, as shown in Fig. 11. Finally, the objects are placed in the workpiece placement area, as illustrated in Fig. 12 and Fig. 13.
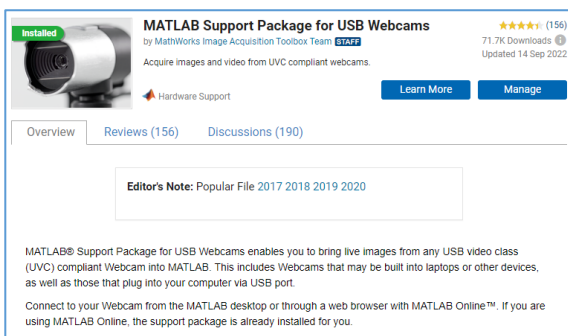

Fig. 9. Add-On explorer of MATLAB support package for USB webcams.
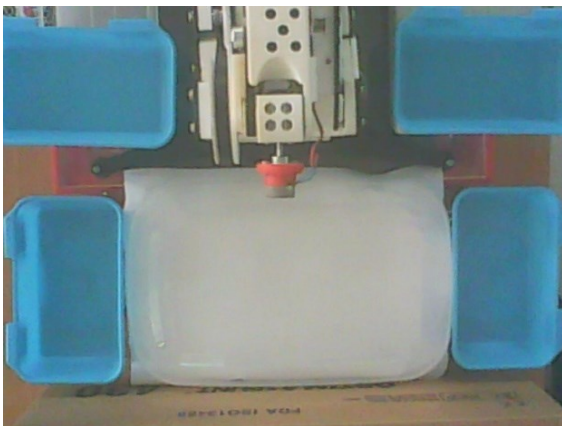

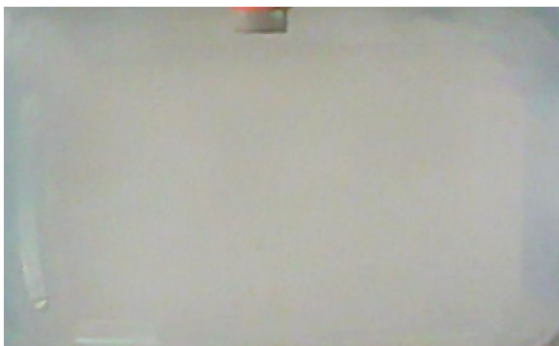Fig. 10. Top view work area when there are no components present

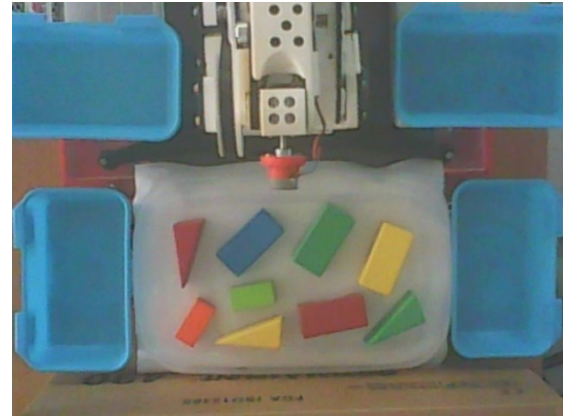Fig. 11. work area when there are no components present

Fig. 12. Top view work area with components present

Fig. 13. Work area with components present

Image processing and segmentation are commonly used techniques to identify objects within images. Image processing involves manipulating the original image to enhance its features and make it easier to analyze, such as by converting it to black and white or adjusting its contrast. Image segmentation is the process of dividing the image into meaningful segments or regions, which can involve removing some parts of the image that are not relevant to the analysis from the original image. The effectiveness of image segmentation techniques depends on the specific characteristics of the image being analyzed. For instance, similar research has been applied to image thresholding for the highway visual tracking system [100].

During the preparation process for image analysis, color images are usually converted to grayscale and modified to become black and white. The resulting image is then used for image segmentation to identify the coordinates or locations of the target object. As seen in Fig. 14, the Logitech HD webcam C170 produces images of moderate quality that may appear unclear, but they are still useful for identifying the coordinates or targets of objects within the defined work area. To perform RGB to grayscale conversion in Image Processing, the original color image is first converted to grayscale using the 'rgb2gray' function. After that, the 'im2bw' function is applied to the grayscale image using a threshold value to convert it into a binary image. However, image segmentation may not always result in the complete identification of all objects in the image. In this example, only three out of the ten expected objects were successfully identified.
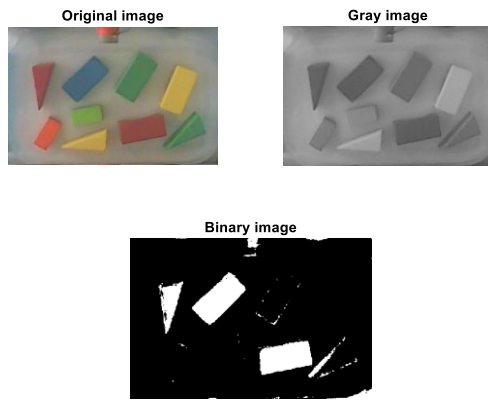
Fig. 14. Results of utilizing the grayscale adjustment technique in the image preparation procedure, converting an image to black and white.

According to Fig. 14, the image segmentation did not produce the expected results due to background problems in the work piece placement area. The gray level range, as seen in Fig. 15, is between 140-170, which overlaps with different colors and object shadows. Additionally, there are objects with varying gray values, which makes it challenging to separate using general commands or filters without special conditions. As a result, a complete black and white image suitable for image segmentation was not obtained.

To address this issue, this research proposes using an expert system to manage data and implement the preparation process of single and dual image processing techniques, which will be discussed in the upcoming section.
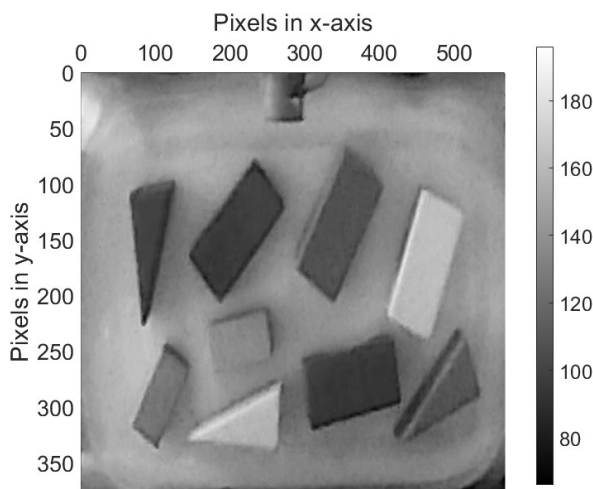

Fig. 15. Results of utilizing the grayscale adjustment technique in the image preparation procedure.

B. Image Segmentation

This section outlines the process of designing image segmentation of images. The first step involves creating a black and white image and determining the object's size coordinates, after which the image is bordered, as demonstrated in Fig. 16. The next step involves identifying the frame that covers the object by converting the image to black and white and then detecting objects in the binary image using blob analysis. The system design conditions are stored in the blob_analysis variable using the function blob_analysis = vision.BlobAnalysis('MinimumBlobArea', 2700, 'MaximumBlobArea', 10000), which sets the minimum

value to 2,700 and the maximum value to 10,000 and saves the index value in the bboxes variable. Using the command [areas, centroids, bboxes] = step(blob_analysis, binary_img), where the binary_img variable is a predesigned black and white image, the resulting bboxes variable provides the value of areas$_{(x_{obj}, y_{obj})}$, which returns the x_{obj}, y_{obj} coordinates of the top corner of the object within the image, and centroids$_{(x_{obj}, y_{obj})}$, which is the length of the object within the image itself.
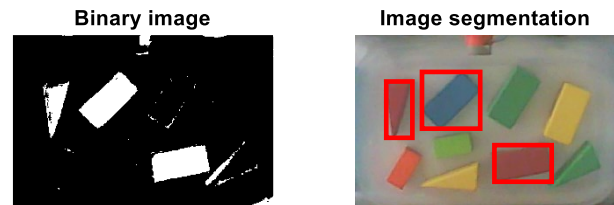

Fig. 16. Outcome of an image in black and white to image segmentation.

One can obtain the coordinates of the CG in the image by using (1) and (2).

$$CG_x(x_{obj}) = x_{obj} + \frac{\text{centroids}_{x_{obj}}}{2} \tag{1}$$

$$CG_y(y_{obj}) = y_{obj} + \frac{\text{centroids}_{y_{obj}}}{2} \tag{2}$$

IV. PREPARATION PROCESS OF IMAGE PROCESSING

In this section, we will discuss the preparation process for image processing, as presented in the paper. The preparation process includes two conditions for image processing: the preparation process of single image processing and the preparation process of dual image processing.

A. Preparation Process of Single Image Processing

This section focuses on the design of the preparation process for single image processing, which involves designing the rules of an expert system presented as equation as in (3).

$$\begin{aligned} &IF\ (RGB\ of\ image\ input \\ &\geq \min of\ RGB\ in\ background)\ and \\ &(RGB\ of\ image\ input \\ &\leq \max of\ RGB\ in\ background) \\ &THEN\ (RGB\ of\ image\ input\ is\ 0). \end{aligned} \tag{3}$$

The rules outlined in (3) can be translated into a program code, as shown in (4).

$$\begin{aligned} &IF\ (input\ R_{x,y} \geq \min of\ R_{x,y}\ in\ background)\ and \\ &(input\ G_{x,y} \geq \min of\ G_{x,y}\ in\ background)\ and \\ &(input\ B_{x,y} \geq \min of\ B_{x,y}\ in\ background)\ and \\ &(input\ R_{x,y} \leq \max of\ R_{x,y}\ in\ background)\ and \\ &(input\ G_{x,y} \leq \max of\ G_{x,y}\ in\ background)\ and \\ &(input\ B_{x,y} \leq \max of\ B_{x,y}\ in\ background) \\ &THEN\ (R_{x,y}\ of\ image\ input\ is\ 0)\ and \\ &(G_{x,y}\ of\ image\ input\ is\ 0)\ and \\ &(B_{x,y}\ of\ image\ input\ is\ 0). \end{aligned} \tag{4}$$

Fig. 17 shows a sample image in which the RGB color value of the floor of the object placement was measured. The measurement revealed that the plates had RGB color values of R ranging from 105-180, G ranging from 115-180, and B ranging from 95-180.
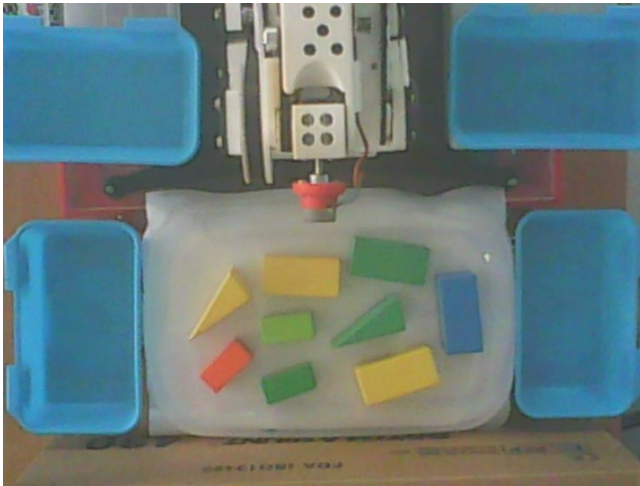
Fig. 17. Images Utilized in the Experiment as Samples.

After cropping the original image in Fig. 18, the expert system method of (4) is used to modify the image. Following that, the image is converted to black and white using the conditions designed according to rule (4).

The im2bw(I, level) command is used to modify the image data. This command converts the grayscale image I to a binary image BW. It replaces all pixels in the input image with a luminance greater than the level with the value 1 (white) and replaces all other pixels with the value 0 (black).

The range of level is relative to the signal levels possible for the image's class. In this research, a level value of 0.2 corresponds to an intensity value halfway between the minimum and maximum value of the class of image files used in this research.

B. Preparation Process of Dual Image Processing

The preparation process of dual image processing is a proposed technique that utilizes the conditions of the original image before the work was placed and the image with the workpiece placed on it, as shown in Fig. 11 and Fig. 13. The technique involves comparing the RGB values in the x, y coordinates of both images to determine whether they are within the specified range in Fig. 11, while maintaining the size of the RGB colors in the image. If the conditions are not met, the values are set to 0. The expert system can be designed using (5).

$$IF \ (RGB \ of \ image \ input \\ \leq [RGB \ of \ background \\ + range \ of \ upper]) \ and$$

$$(RGB \ of \ image \ input \\ \geq [RGB \ of \ background \\ - range \ of \ lowwer]) \quad (5)$$

$$THEN \ (RGB \ of \ image \ input \ \ is \ 0).$$
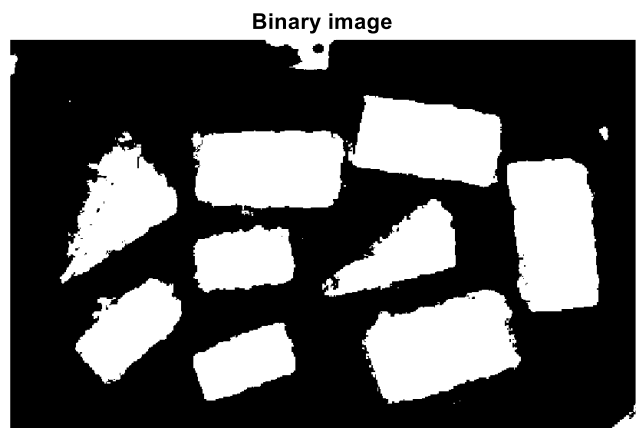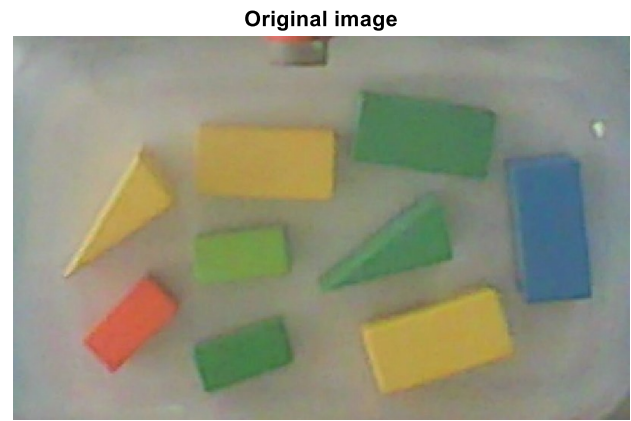
Original image

Binary image

Fig. 18. Outcome of employing the single image technique in the image preparation process, converting an image to black and white.

The rules in (5) can be expressed as a program condition, which is shown in (6).

$$IF \ \big(input \ R_{x,y} \ \leq \big[R_{x,y} \ in \ background \\ + range \ of \ upper\big]\big) and$$
$$\big(input \ R_{x,y} \ \geq \big[R_{x,y} \ in \ background \\ - range \ of \ lowwer\big]\big) and$$
$$\big(input \ G_{x,y} \ \leq \big[G_{x,y} \ in \ background \\ + range \ of \ upper\big]\big) and$$
$$\big(input \ G_{x,y} \ \geq \big[G_{x,y} \ in \ background \\ - range \ of \ lowwer\big]\big) and \quad (6)$$
$$\big(input \ B_{x,y} \ \leq \big[B_{x,y} \ in \ background \\ + range \ of \ upper\big]\big) and$$
$$\big(input \ B_{x,y} \ \geq \big[B_{x,y} \ in \ background \\ - range \ of \ lowwer\big]\big) and$$
$$THEN \ \big(R_{x,y} \ of \ image \ input \ is \ 0\big) \ and$$
$$\big(G_{x,y} \ of \ image \ input \ is \ 0\big) \ and$$
$$\big(B_{x,y} \ of \ image \ input \ is \ 0\big).$$

The RGB color range of the floor of the object holder in the sample from Fig. 16 has been measured. The upper range can be set to 20 and the lower range can be set to 79, and both values are suitable for the experiments conducted in this study.
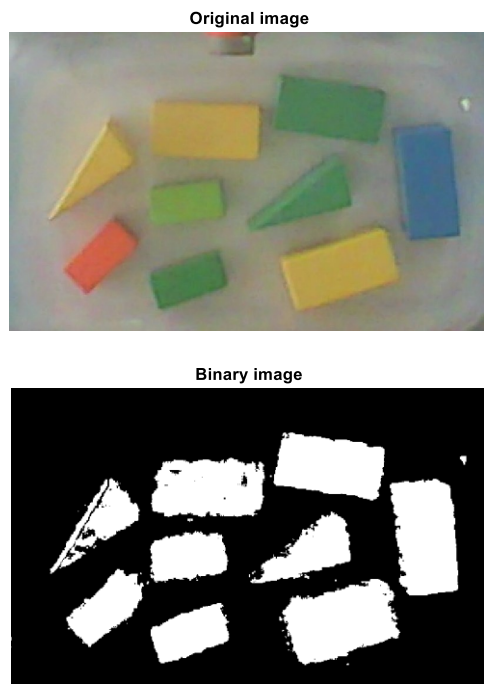
Original image

Binary image

Fig. 19. Outcome of employing the dual image technique in the image preparation process, converting an image to black and white.

When cropping the original image to produce Fig. 19, the expert system method was applied using Equation (6) to modify the image. The resulting image was then converted to black and white using the im2bw(I, level) command, with a level value of 0.2.

This process was conducted in accordance with the conditions designed in rule (5) of the preparation process of dual image processing test, as well as the preparation process of a single image processing test.

V. OBJECT DETECTION USING RESNET-18

A. Architecture and Environment of the System

To identify objects or details within an image for inspection purposes, various techniques may be employed. In some cases, the use of optimized image processing techniques [101] can help determine the coordinates or areas to be focused on in the image. This can involve the use of CNN algorithms [102] or deep learning [103] to help extract the necessary information needed for object identification. Currently, many ready-made algorithms [104], [105] are available for image processing, which can be used to reduce design time for image analysis. The image classification system utilized in this study is based on convolutional neural network (CNN) and its architecture is presented in Fig. 20. The system consists of two main components.
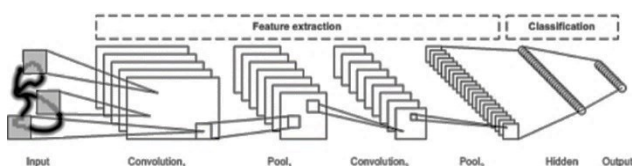
Fig. 20. The architecture and procedure of convolutional neural networks.

1. Feature extraction is an image processing technique that extracts the salient features of objects in the image, such as

edges, contours, and creates a model. Then, the extracted feature information is taken as input and processed by the neural network in the following stage.

2. Neural network for classification is used to classify the images according to the model groups that have been trained.

In this research, the ResNet-18 architecture was utilized, which is a learning framework that enhances the effectiveness of deep residual network training. When working with a significant number of layers, vanishing gradients may become an issue. However, ResNet addresses this by using shortcut methods, bypassing certain network layers. The ResNet-18 model was implemented, and its structure is presented in Fig. 22, with the Add-On explorer depicted in Fig. 21.
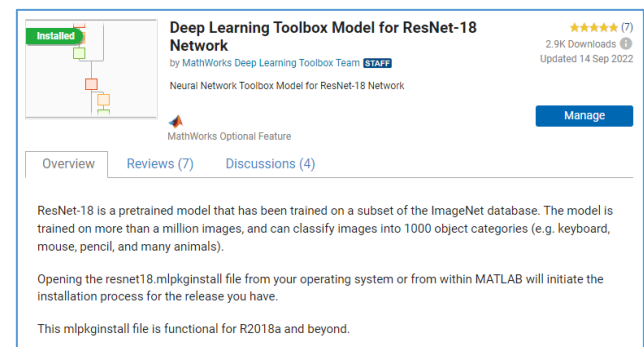
Fig. 21. Add-On explorer of the deep learning toolbox model for ResNet-18 network

B. system design of ResNet-18

The classification system's working design comprises the following steps:

1. The input consists of image data of workpieces that can be used for training, validation, testing, and prediction. The number of input images affects the processing because each sample of the workpiece block is processed separately. This research deals with two groups of workpiece blocks. Group 1 comprises two types, namely, triangular and rectangular. Group 2 includes six types, divided into six colors, four of which are blue, green, orange, red, verdant, and yellow. Each category in the two groups has a varying number of images. To equalize the number of images for each class in the training data, we introduced a technique called oversampling. Deep learning can become challenging if the training data's amount varies across classes, as shown in Fig. 23. To address this, an oversampling technique was used to balance the number of images for each class in the training data.

2. Convolution is a layer that processes input image data using a specified kernel size to obtain a feature map. This process detects straight, curved, and beveled edges in the images, allowing the system to create a model.

3. Max pooling is a layer that reduces the size of the feature map by half.

4. The fully-connected layer (FC) organizes the multidimensional data from the previous layer into a 1-dimensional vector (called Flatten) and feeds it to the neural network layer. In this layer, the input and weights act as

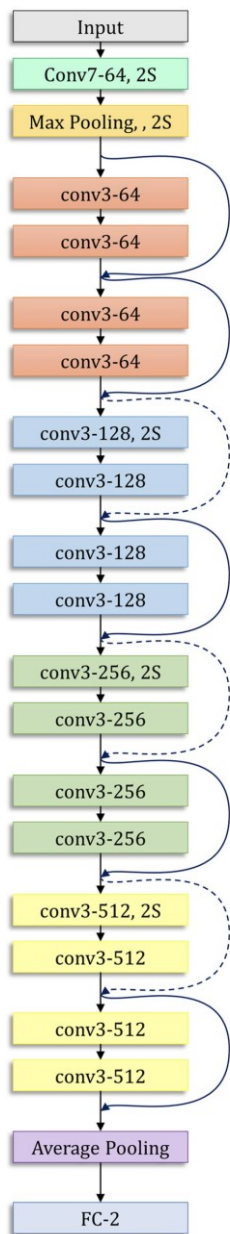classification, providing output results to predict the type of workpiece block depicted in the input image.

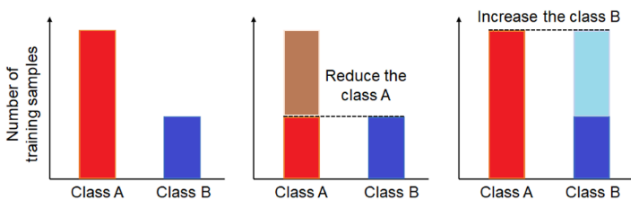
Fig. 22. Design of the ResNet-18 model architecture.

Fig. 23. Oversampling technique.

C. The Workflow for Machine Learning

The system is trained on two groups of workpiece block datasets, enabling it to learn and distinguish between various types of workpiece blocks using a feature extraction and modeling system. The resulting model can then be utilized to recognize and predict the type of block from images captured by the Logitech HD webcam C170 with accuracy. Deep learning is used as the machine learning process, as depicted in Fig. 24.
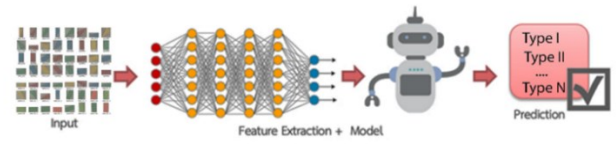

Fig. 24. The learning procedure of the classification system.

In this research, the detection learning process was developed using image recognition as a tool to teach models to analyze images. The model was trained using two groups of work blocks, which were separated into two different trainings: color training and shape training.

In the color training group from Fig. 25, there were 43 blue images, 53 green images, 11 orange images, 42 red images, 11 verdant images, and 54 yellow images. To ensure an equal number of images for each class in the training data, oversampling was done, resulting in 38 images per group as shown in Fig. 26. The GUI data training in color training was displayed in Fig. 27 during the ResNet-18 method training process. Once the training was completed, the mean training and validation accuracy in color training were computed and displayed in Fig. 28, indicating the accuracy in each category.
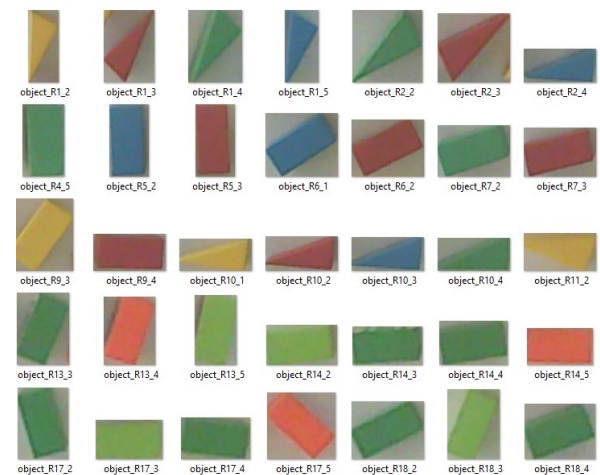

Fig. 25. Examples of image data employed in classification
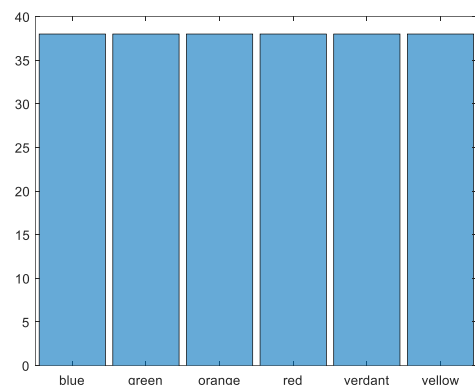

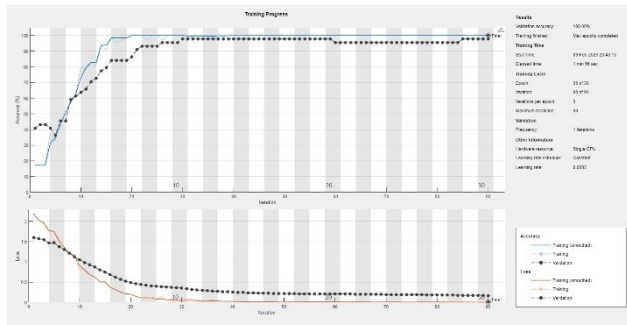Fig. 26. Outcomes of the oversampling technique in color training.

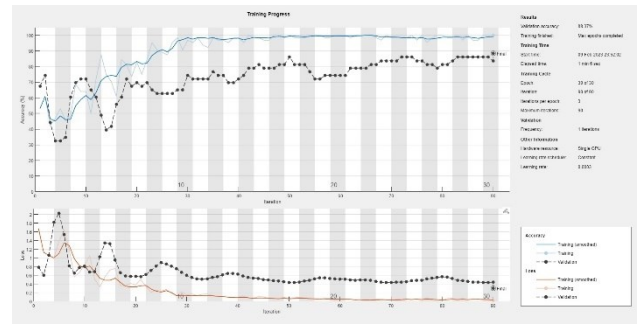Fig. 27. GUI data training in color training.

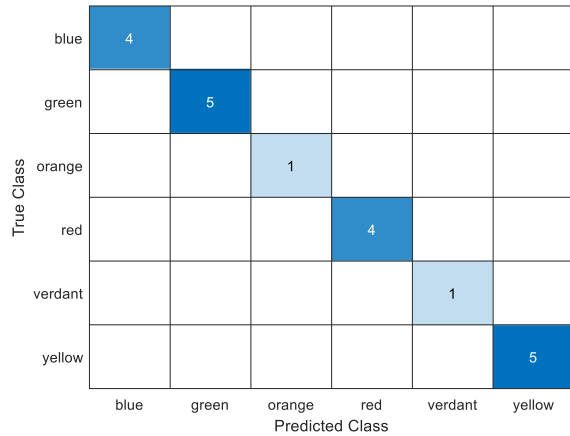Fig. 30. GUI data training in shape training.

Fig. 28. Compute the mean training and validation accuracy in color training.
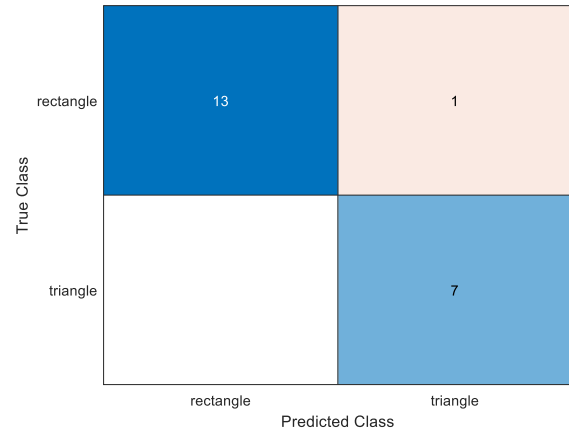

Fig. 31. Compute the mean training and validation accuracy in shape training.

In the shape training group's training process using the ResNet-18 method, two shapes were extracted from the example shown in Fig. 25. These included 142 rectangles and 69 triangles. To ensure an equal number of images for each class in the training data, oversampling was performed, resulting in 99 images for each group as displayed in Fig. 29. Fig. 30 shows the GUI data training in shape training during the ResNet-18 method training process. Once the training was completed, the mean training and validation accuracy in shape training were computed and displayed in Fig. 31, indicating the accuracy in each category.
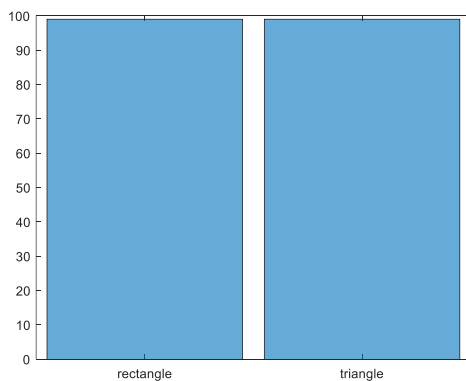
This research utilized a dataset of 211 workpiece block images to teach the model to recognize and differentiate between different types. Image recognition was employed as a tool to predict results. During the testing process, the object was cropped using bounding box information, and the image was resized to 224×224 pixels. The predict command was then used to retrieve the net data from the system's training data, which had learned the color value and shape of the object. Finally, the prediction results were checked against category classes, and the prediction text was recorded in the class labels.

VI.   EXPERIMENTAL RESULTS

This section presents the results of three experiments: RGB to grayscale conversion for image processing, single image processing, and dual image processing. To verify the images, the original files, black and white images, color images with the background removed and the subject covered, and original images with the object covered were analyzed to determine the workpiece type and CG point. The next section will detail these results.

Fig. 29. Outcomes of the oversampling technique in shape training.

The experiment identified two different situations in the presented sample, as illustrated in Fig. 32 and Fig. 33, where the placement and number of workpieces in the workpiece tray differed in the system designed for RGB to grayscale conversion for image processing, single image processing, and dual image processing.
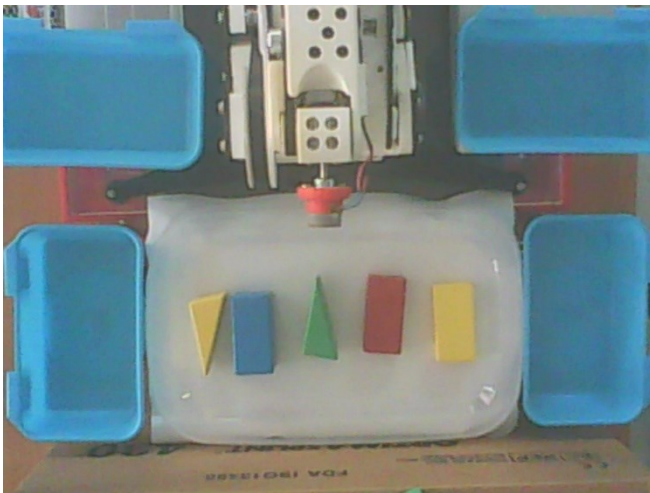
Fig. 32. The work area in 5 parts for experimental.

Fig. 33. The work area in 9 parts for experimental.

A. RGB to Grayscale Conversion to Image Processing

The results from the first test in the experimental study on RGB to grayscale conversion for image processing, which aimed to prepare for single image processing using the RGB to grayscale conversion technique and utilized images from Fig. 34, Fig. 35, Fig. 36, and Fig. 37, indicated that the basic method used in the test had limited ability to distinguish between the workpiece tray and the parts. Specifically, with the images from Fig. 32 and Fig. 33, this technique was able to successfully isolate only 1 out of 5 and 1 out of 10 specimens, respectively.

Technically, by transforming the original RGB image to grayscale and then to black and white, the program can efficiently identify the color and object shapes using ResNet-18, and accurately determine the edges of the object and CG values within the image. However, the program has limitations due to the difference in color levels between the tested part and the workpiece tray, with grayscale values in the range of 140-180, while the grayscale value of the part image is either 0-160 or 180-255. Thus, this technique may not be suitable when there is a diverse range of colors in the workpiece.

Fig. 34. The results of test I in grayscale adjustment technique to image processing experimental.

Fig. 35. Final results of Test I in grayscale adjustment technique to image processing experimental.
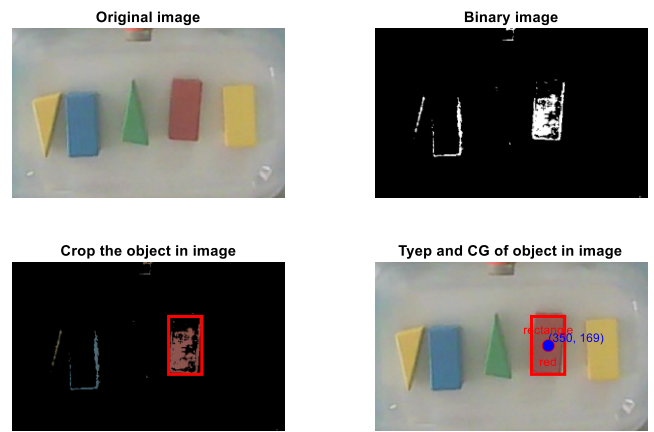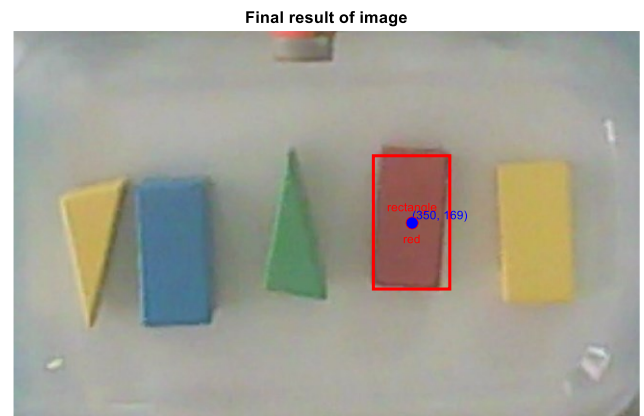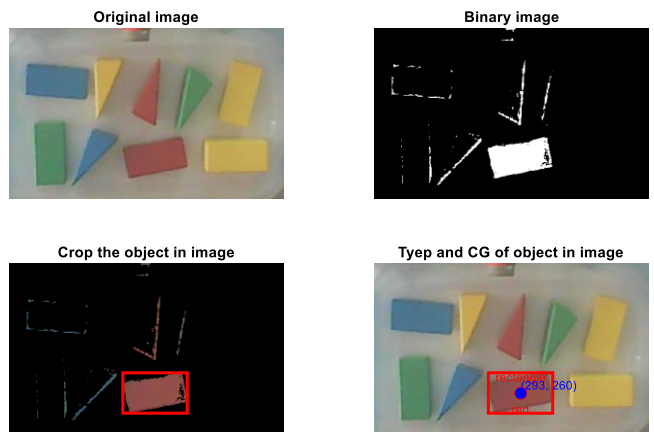

Fig. 36. The results of test II in grayscale adjustment technique to image processing experimental.
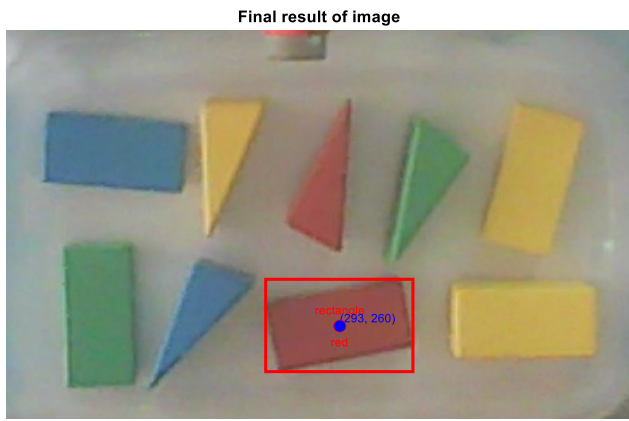
Fig. 37. Final results of Test II in grayscale adjustment technique to image processing experimental.

B. Single Image Processing

The second test of experiments focuses on the preparation process of single image processing using images from Fig. 32 and Fig. 33, as depicted in Fig. 38, Fig. 39, Fig. 40, and Fig. 41. The results demonstrate the program's ability to extract the color range between the background and the workpiece and convert the original image into black and white image, accurately separating the edges of the object and CG values within the image with a 100% success rate for objects located in the workpiece tray. The ResNet-18 algorithm efficiently identifies the color and object shapes, and the results are accurate in all tested photographs.

Although some images have devices in the background, such as the handle head or reflected light, that can affect the completeness of the image cutting, the program can be edited by setting the maximum and minimum values of the space within the object and adding more rules to cut off the RGB color group.

Fig. 38. The results of test I in a single image processing experimental.

Fig. 39. Final results of Test I in a single image processing experiment.

Fig. 40. The results of test II in a single image processing experimental.

Fig. 41. Final results of Test II in a single image processing experiment

C. Dual Image Processing

The third test in the experimental study focused on the preparation process of dual image processing using images from Fig. 32 and Fig. 33, and the results are presented in Fig. 42, Fig. 43, Fig. 44, and Fig. 45. Similar to the single image processing results, image processing techniques were utilized, but with additional capabilities. The program was able to extract the color range between the background and the color of the workpiece, resulting in cropping the original image into a black and white image that accurately separated the edges of the object and CG values within the image, with a 100% success rate for objects located in the workpiece tray.

Furthermore, the program was able to use image position information to determine the location of the object within the

image and specify the CG value. By using ResNet-18, the program accurately identified the color and shape of the object in all photographic tests, even with reflections that were not completely removed from the original image. Moreover, the program was capable of cutting the background image and the head of the robot gripper, expanding its capabilities beyond that of single image processing. Overall, dual image processing has more advanced capabilities than single image processing
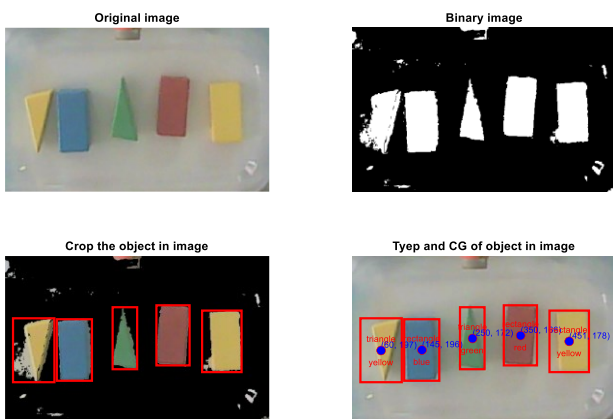

Fig. 42. The results of test I in dual image processing experimental.

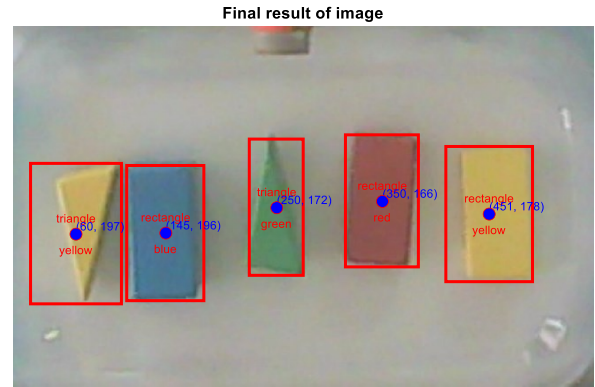
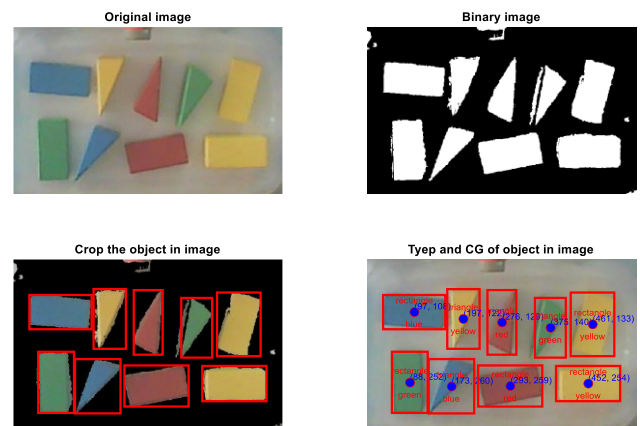Fig. 43. Final results of Test I in the dual image processing experiment.

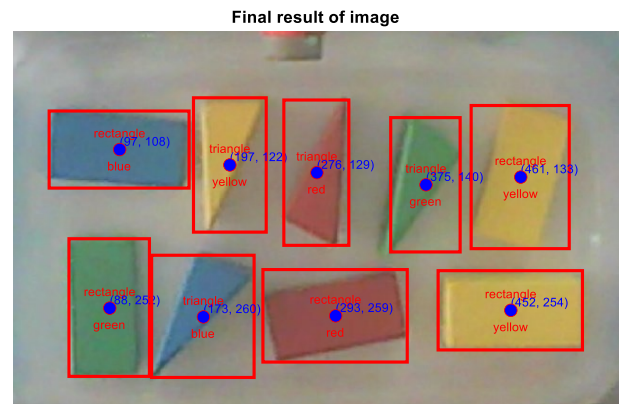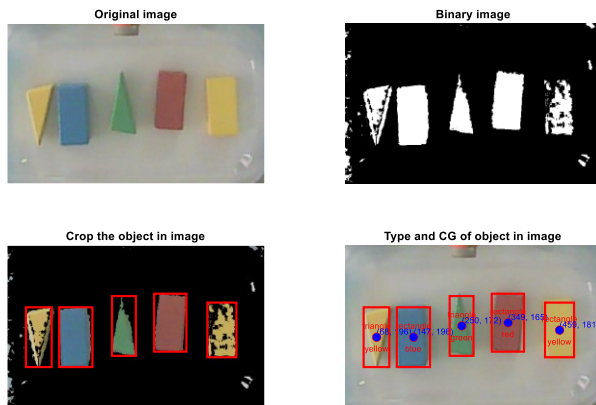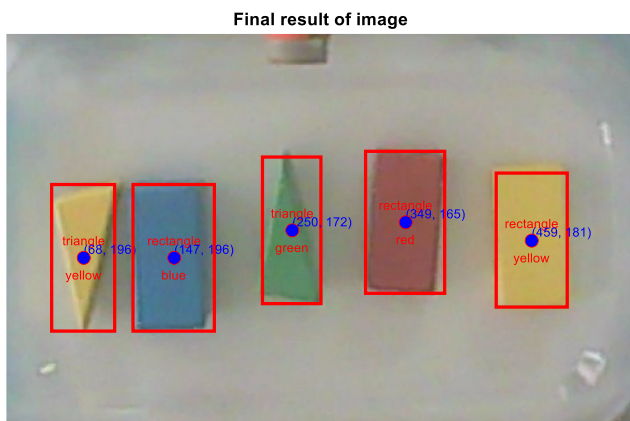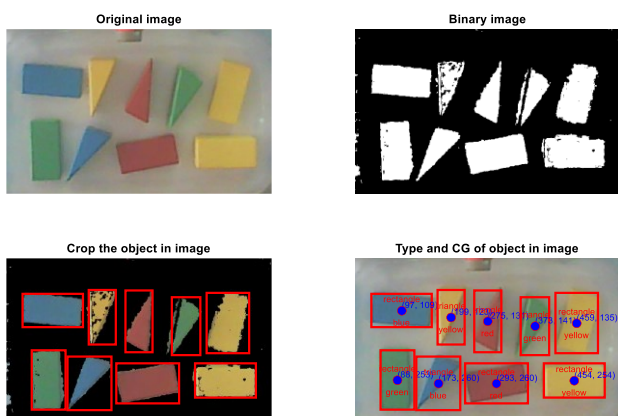Fig. 44. The results of test II in dual image processing experimental.
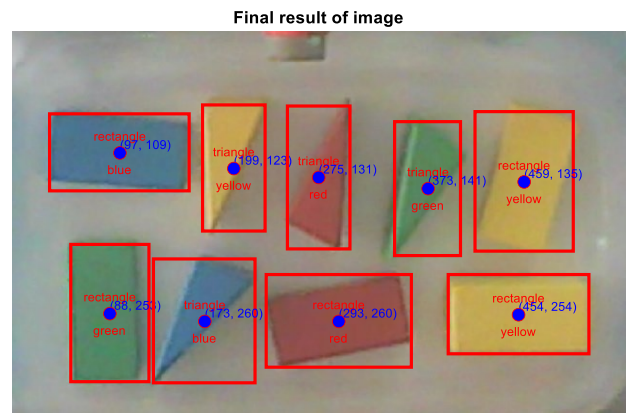
Fig. 45. Final results of Test II in the dual image processing experiment.

D. Summary of the results

The experimental results demonstrate the superiority of the dual image processing technique over both RGB to grayscale conversion and single image processing. The program achieved a 100% success rate in accurately separating the edges of the object and CG values within the image, while also identifying the color and shape of the object using ResNet-18. The program was able to use image position information to determine the location of the object within the image and specify the CG value. Additionally, the program was capable of cutting the background image and the head of the robot gripper, expanding its capabilities beyond that of single image processing. As a result, the dual image processing technique provides advanced capabilities for object recognition and can be a valuable tool in industrial automation applications.

However, both single and dual image processing methods have limitations and disadvantages. Single image processing requires checking the light and color tone within the image to cut off other objects that need to be removed, which may require many conditions. On the other hand, dual image processing can extract background images and objects if there is a picture in the reference, making the conditions for cutting objects within the image less, but may become problematic if the light is shifted.

To solve the aberration image problem, the background clipping condition may need to be set as the nature of the index data or may use NN to solve the problem, depending on the amount of information or conditions that arise to create a boundary of conditions.

VII. CONCLUSION

In summary, this study examined the use of RGB to grayscale conversion, single image processing, and dual image processing methods for object recognition in industrial automation applications. The findings suggest that the dual image processing technique offers superior capabilities in accurately identifying object edges, determining CG values, and cutting background images and gripper heads. However, single image processing may still have advantages in certain scenarios with sufficient image information and favorable lighting conditions. Overall, this study provides valuable insights into the strengths and limitations of different object recognition techniques for industrial automation applications. Future research could focus on further improvements and

optimization of these methods, including the possibility of separating objects into boxes of each type and converting the image's coordinate data into the coordinates of the robot's working area to design a point-to-point robot path. These areas may require further investigation in future research.

REFERENCES

[1] S. Wan and S. Goudos, "Faster R-CNN for multi-class fruit detection using a robotic vision system," *Computer Networks*, vol. 168, p. 107036, 2020.

[2] M. Halstead, C. McCool, S. Denman, T. Perez, and C. Fookes, "Fruit quantity and ripeness estimation using a robotic vision system," *IEEE Robotics and Automation Letters*, vol. 3, no. 4, pp. 2995-3002, 2018.

[3] A. Gongal, M. Karkee, and S. Amatya, "Apple fruit size estimation using a 3D machine vision system," *Information Processing in Agriculture*, vol. 5, no. 4, pp. 498-503, 2018.

[4] H. A. Williams et al., "Robotic kiwifruit harvesting using machine vision, convolutional neural networks, and robotic arms," *Biosystems Engineering*, vol. 181, pp. 140-156, 2019.

[5] J. J. Zhuang et al., "Detection of orchard citrus fruits using a monocular machine vision-based method for automatic fruit picking applications," *Computers and Electronics in Agriculture*, vol. 152, pp. 64-73, 2018.

[6] Y. Tang et al., "Recognition and localization methods for vision-based fruit picking robots: A review," *Frontiers in Plant Science*, vol. 11, p. 510, 2020.

[7] Z. Wang, J. Underwood, and K. B. Walsh, "Machine vision assessment of mango orchard flowering," *Computers and Electronics in Agriculture*, vol. 151, pp. 501-511, 2018.

[8] S. D. Kumar et al., "A microcontroller based machine vision approach for tomato grading and sorting using SVM classifier," *Microprocessors and Microsystems*, vol. 76, p. 103090, 2020.

[9] M. T. Habib et al., "Machine vision based papaya disease recognition," *Journal of King Saud University-Computer and Information Sciences*, vol. 32, no. 3, pp. 300-309, 2020.

[10] E. Mavridou et al., "Machine vision systems in precision agriculture for crop farming," *Journal of Imaging*, vol. 5, no. 12, p. 89, 2019.

[11] A. Wang, W. Zhang, and X. Wei, "A review on weed detection using ground-based machine vision and image processing techniques," *Computers and Electronics in Agriculture*, vol. 158, pp. 226-240, 2019.

[12] L. Li, X. Mu, S. Li, and H. Peng, "A review of face recognition technology," *IEEE Access*, vol. 8, pp. 139110-139120, 2020.

[13] M. Z. Khan, S. Harous, S. U. Hassan, M. U. G. Khan, R. Iqbal, and S. Mumtaz, "Deep unified model for face recognition based on convolution neural network and edge computing," *IEEE Access*, vol. 7, pp. 72622-72633, 2019.

[14] M. Sajjad, M. Nasir, K. Muhammad, S. Khan, Z. Jan, A. K. Sangaiah, et al., "Raspberry Pi assisted face recognition framework for enhanced law-enforcement services in smart cities," *Future Generation Computer Systems*, vol. 108, pp. 995-1007, 2020.

[15] A. Jha, "Classroom attendance system using facial recognition system," *The International Journal of Mathematics, Science, Technology, and Management*, vol. 2, no. 3, pp. 4-7, 2007.

[16] F. Tabassum, M. I. Islam, R. T. Khan, and M. R. Amin, "Human face recognition with combination of DWT and machine learning," *Journal of King Saud University-Computer and Information Sciences*, vol. 34, no. 3, pp. 546-556, 2022.

[17] R. I. Bendjillali, M. Beladgham, K. Merit, and A. Taleb-Ahmed, "Illumination-robust face recognition based on deep convolutional neural networks architectures," *Indonesian Journal of Electrical Engineering and Computer Science*, vol. 18, no. 2, pp. 1015-1027, 2020.

[18] H. Ling, J. Wu, L. Wu, J. Huang, J. Chen, and P. Li, "Self residual attention network for deep face recognition," *IEEE Access*, vol. 7, pp. 55159-55168, 2019.

[19] V. T. Dang, N. Nguyen, H. V. Nguyen, H. Nguyen, L. Van Huy, V. T. Tran, and T. H. Nguyen, "Consumer attitudes toward facial recognition payment: an examination of antecedents and outcomes," *International Journal of Bank Marketing*, vol. 40, no. 3, pp. 511-535, 2022.

[20] A. Alzu'bi, F. Albalas, T. Al-Hadhrami, L. B. Younis, and A. Bashayreh, "Masked face recognition using deep learning: A review," *Electronics*, vol. 10, no. 21, pp. 2666, 2021.

[21] T. Zhou, D. P. Fan, M. M. Cheng, J. Shen and L. Shao, "RGB-D Salient Object Detection: A Survey," *Computational Visual Media*, vol. 7, pp. 37-69, 2021.

[22] A. Suhail, M. Jayabalan and V. Thiruchelvam, "Convolutional Neural Network Based Object Detection: A Review," *Journal of Critical Reviews*, vol. 7, no. 11, pp. 786-792, 2020.

[23] S. S. A. Zaidi, M. S. Ansari, A. Aslam, N. Kanwal, M. Asghar and B. Lee, "A Survey of Modern Deep Learning Based Object Detection Models," *Digital Signal Processing*, vol. 115, p. 103514, 2022.

[24] W. Zhao, W. Ma, L. Jiao, P. Chen, S. Yang and B. Hou, "Multi-Scale Image Block-Level F-CNN for Remote Sensing Images Object Detection," *IEEE Access*, vol. 7, pp. 43607-43621, 2019.

[25] S. Zhang, Y. Wu, C. Men and X. Li, "Tiny YOLO Optimization Oriented Bus Passenger Object Detection," *Chinese Journal of Electronics*, vol. 29, no. 1, pp. 132-138, 2020.

[26] X. Chen, H. Li, Q. Wu, K. N. Ngan and L. Xu, "High-Quality R-CNN Object Detection Using Multi-Path Detection Calibration Network," *IEEE Transactions on Circuits and Systems for Video Technology*, vol. 31, no. 2, pp. 715-727, 2021.

[27] A. Kuznetsova et al., "The Open Images Dataset V4: Unified Image Classification, Object Detection, and Visual Relationship Detection at Scale," *International Journal of Computer Vision*, vol. 128, no. 7, pp. 1956-1981, 2020.

[28] X. Zhao, P. Sun, Z. Xu, H. Min and H. Yu, "Fusion of 3D LIDAR and Camera Data for Object Detection in Autonomous Vehicle Applications," *IEEE Sensors Journal*, vol. 20, no. 9, pp. 4901-4913, 2020.

[29] M. Shirpour, N. Khairdoost, M. Bauer and S. Beauchemin, "Traffic Object Detection and Recognition Based on the Attentional Visual Field of Drivers," *IEEE Transactions on Intelligent Vehicles*, 2021.

[30] Z. Zou, K. Chen, Z. Shi, Y. Guo and J. Ye, "Object Detection in 20 Years: A Survey," *Proceedings of the IEEE*, 2023.

[31] A. N. Hidayah, S. A. Radzi, N. A. Razak, W. H. M. Saad, Y. C. Wong, and A. A. Naja, "Disease Detection of Solanaceous Crops Using Deep Learning for Robot Vision," *Journal of Robotics and Control (JRC)*, vol. 3, no. 6, pp. 790-799, 2022.

[32] C. D. Vo, D. A. Dang, and P. H. Le, "Development of Multi-Robotic Arm System for Sorting System Using Computer Vision," *Journal of Robotics and Control (JRC)*, vol. 3, no. 5, pp. 690-698, 2022.

[33] M. I. Rusydi, A. Novira, T. Nakagome, J. Muguro, R. Nakajima, W. Njeri, et al., "Autonomous Movement Control of Coaxial Mobile Robot based on Aspect Ratio of Human Face for Public Relation Activity Using Stereo Thermal Camera," *Journal of Robotics and Control (JRC)*, vol. 3, no. 3, pp. 361-373, 2022.

[34] X. Zheng, Q. Lei, R. Yao, Y. Gong, and Q. Yin, "Image segmentation based on adaptive K-means algorithm," *EURASIP Journal on Image and Video Processing*, vol. 2018, no. 1, pp. 1-10, 2018.

[35] R. Srikanth and K. Bikshalu, "Multilevel thresholding image segmentation based on energy curve with harmony Search Algorithm," *Ain Shams Engineering Journal*, vol. 12, no. 1, pp. 1-20, 2021.

[36] G. Aletti, A. Benfenati, and G. Naldi, "A semiautomatic multi-label color image segmentation coupling Dirichlet problem and colour distances," *Journal of Imaging*, vol. 7, no. 10, pp. 208, 2021.

[37] H. Costa, G. M. Foody, and D. S. Boyd, "Supervised methods of image segmentation accuracy assessment in land cover mapping," Remote Sensing of Environment, vol. 205, pp. 338-351, 2018.

[38] M. D. Hossain and D. Chen, "Segmentation for Object-Based Image Analysis (OBIA): A review of algorithms and challenges from remote sensing perspective," *ISPRS Journal of Photogrammetry and Remote Sensing*, vol. 150, pp. 115-134, 2019.

[39] Y. Xiao, L. Daniel, and M. Gashinova, "Image segmentation and region classification in automotive high-resolution radar imagery," *IEEE Sensors Journal*, vol. 21, no. 5, pp. 6698-6711, 2020.

[40] M. H. Hesamian, W. Jia, X. He, and P. Kennedy, "Deep learning techniques for medical image segmentation: achievements and challenges," *Journal of digital imaging*, vol. 32, pp. 582-596, 2019.

[41] M. Z. Alom, C. Yakopcic, M. Hasan, T. M. Taha, and V. K. Asari, "Recurrent residual U-Net for medical image segmentation," *Journal of Medical Imaging*, vol. 6, no. 1, pp. 014006-014006, 2019.

[42] A. Sinha and J. Dolz, "Multi-scale self-guided attention for medical image segmentation," *IEEE Journal of Biomedical and Health Informatics*, vol. 25, no. 1, pp. 121-130, 2021.

[43] N. Siddique, S. Paheding, C. P. Elkin, and V. Devabhaktuni, "U-net and its variants for medical image segmentation: A review of theory and applications," *IEEE Access*, vol. 9, pp. 82031-82057, 2021.

[44] A. Desiani, B. Suprihatin, S. Yahdin, A. I. Putri, and F. R. Husein, "Bi-path Architecture of CNN Segmentation and Classification Method for Cervical Cancer Disorders Based on Pap-smear Images," *IAENG International Journal of Computer Science*, vol. 48, no. 3, 2021.

[45] D. Marmanis, K. Schindler, J. D. Wegner, S. Galliani, M. Datcu, and U. Stilla, "Classification with an edge: Improving semantic image segmentation with boundary detection," *ISPRS Journal of Photogrammetry and Remote Sensing*, vol. 135, pp. 158-172, 2018.

[46] G. Sun, X. Jia, and T. Geng, "Plant diseases recognition based on image processing technology," *Journal of Electrical and Computer Engineering*, vol. 2018, 2018.

[47] S. Wang, D. M. Yang, R. Rong, X. Zhan, and G. Xiao, "Pathology image analysis using segmentation deep learning algorithms," *The American Journal of Pathology*, vol. 189, no. 9, pp. 1686-1698, 2019.

[48] F. Munawar, S. Azmat, T. Iqbal, C. Grönlund, and H. Ali, "Segmentation of lungs in chest X-ray image using generative adversarial networks," *IEEE Access*, vol. 8, pp. 153535-153545, 2020.

[49] S. M. Anwar, M. Majid, A. Qayyum, M. Awais, M. Alnowami, and M. K. Khan, "Medical image analysis using convolutional neural networks: a review," *Journal of Medical Systems*, vol. 42, pp. 1-13, 2018.

[50] F. Shi, J. Wang, J. Shi, Z. Wu, Q. Wang, Z. Tang, et al., "Review of artificial intelligence techniques in imaging data acquisition, segmentation, and diagnosis for COVID-19," *IEEE Reviews in Biomedical Engineering*, vol. 14, pp. 4-15, 2021.

[51] A. Mohan and S. Poobal, "Crack detection using image processing: A critical review and analysis," *Alexandria Engineering Journal*, vol. 57, no. 2, pp. 787-798, 2018.

[52] P. K. Dash, S. Mishra, M. A. Salama, and A. C. Liew, "Classification of power system disturbances using a fuzzy expert system and a Fourier linear combiner," *IEEE Transactions on Power Delivery*, vol. 15, no. 2, pp. 472-477, Apr. 2000.

[53] K. Kunhimangalam, S. Ovallath, and P. K. Joseph, "A novel fuzzy expert system for the identification of severity of carpal tunnel syndrome," BioMed research international, vol. 2013, 2013.

[54] L. Ali, A. Niamat, J. A. Khan, N. A. Golilarz, X. Xingzhong, A. Noor, and S. A. C. Bukhari, "An optimized stacked support vector machines based expert system for the effective prediction of heart failure," *IEEE Access*, vol. 7, pp. 54007-54014, 2019.

[55] E. Pawan, R. M. Thamrin, W. Widodo, S. H. B. S. H. Bei, and J. J. Luanmasa, "Implementation of Forward Chaining Method in Expert System to Detect Diseases in Corn Plants in Muara Tami District," *International Journal of Computer and Information System (IJCIS)*, vol. 3, no. 1, pp. 27-33, 2022.

[56] B. Lak and J. Rezaeenour, "Maturity assessment of social customer knowledge management (sckm) using fuzzy expert system," *Journal of Business Economics and Management*, vol. 19, no. 1, pp. 192-212, 2018.

[57] B. S. Abu-Nasser and S. S. Abu-Naser, "Cognitive system for helping farmers in diagnosing watermelon diseases," *International Journal of Academic Information Systems Research (IJAISR)*, vol. 2, no. 7, pp. 1-7, 2018.

[58] A. Aristoteles, K. Adhianto, and R. A. Rico Andrian, "Comparative analysis of cow disease diagnosis expert system using Bayesian network and Dempster-Shafer method," *International Journal of Advanced Computer Science and Applications*, vol. 10, no. 4, pp. 227-235, 2019.

[59] M. Raihan, M. M. Hassan, T. Hasan, A. A. M. Bulbul, M. K. Hasan, M. S. Hossain, M. A. Awal, "Development of a smartphone-based expert system for COVID-19 risk prediction at early stage," *IEEE Journal of Biomedical and Health Informatics*, vol. 26, no. 11, pp. 3448-3459, Nov. 2022.

[60] S. Thaker and V. Nagori, "Analysis of fuzzification process in fuzzy expert system," *Procedia Computer Science*, vol. 132, pp. 1308-1316, 2018.

[61] J. Singla, B. Kaur, D. Prashar, S. Jha, G. P. Joshi, K. Park, et al., "A novel fuzzy logic-based medical expert system for diagnosis of chronic kidney disease," *Mobile Information Systems*, vol. 2020, 2020.

[62] E. A. Algehyne, M. L. Jibril, N. A. Algehainy, O. A. Alamri, and A. K. Alzahrani, "Fuzzy neural network expert system with an improved Gini index random forest-based feature importance measure algorithm for early diagnosis of breast cancer in Saudi Arabia," *Big Data and Cognitive Computing*, vol. 6, no. 1, pp. 13, Jan. 2022.

[63] D. K. Bui, T. Nguyen, J. S. Chou, H. Nguyen-Xuan, and T. D. Ngo, "A modified firefly algorithm-artificial neural network expert system for predicting compressive and tensile strength of high-performance concrete," *Construction and Building Materials*, vol. 180, pp. 320-333, May 2018.

[64] F. Schwendicke, T. Golla, M. Dreher, and J. Krois, "Convolutional neural networks for dental image diagnostics: A scoping review," *Journal of Dentistry*, vol. 91, pp. 103226, Mar. 2019.

[65] A. Kamilaris and F. X. Prenafeta-Boldú, "A review of the use of convolutional neural networks in agriculture," *The Journal of Agricultural Science*, vol. 156, no. 3, pp. 312-322, Mar. 2018.

[66] R. H. Abiyev and M. K. S. Ma'aitaH, "Deep convolutional neural networks for chest diseases detection," *Journal of Healthcare Engineering*, vol. 2018, pp. 1-16, Nov. 2018.

[67] L. Santamaria-Granados, M. Munoz-Organero, G. Ramirez-Gonzalez, E. Abdulhay and N. J. I. A. Arunkumar, "Using deep convolutional neural network for emotion detection on a physiological signals dataset (AMIGOS)," *IEEE Access*, vol. 7, pp. 57-67, 2018.

[68] Y. Zhang, P. Tiňo, A. Leonardis, and K. Tang, "A survey on neural network interpretability," *IEEE Transactions on Emerging Topics in Computational Intelligence*, vol. 5, no. 5, pp. 726-742, Oct. 2021.

[69] J. T. Hancock and T. M. Khoshgoftaar, "Survey on categorical data for neural networks," *Journal of Big Data*, vol. 7, no. 1, pp. 1-41, Jan. 2020.

[70] R. Y. Choi, A. S. Coyner, J. Kalpathy-Cramer, M. F. Chiang, and J. P. Campbell, "Introduction to machine learning, neural networks, and deep learning," *Translational Vision Science & Technology*, vol. 9, no. 2, pp. 14, Mar. 2020.

[71] J. X. Chen, P. W. Zhang, Z. J. Mao, Y. F. Huang, D. M. Jiang, and Y. N. Zhang, "Accurate EEG-based emotion recognition on combined features using deep convolutional neural networks," *IEEE Access*, vol. 7, pp. 44317-44328, 2019.

[72] A. B. Nassif, I. Shahin, I. Attili, M. Azzeh, and K. Shaalan, "Speech recognition using deep neural networks: A systematic review," *IEEE Access*, vol. 7, pp. 19143-19165, 2019.

[73] H. Mohsen, E. S. A. El-Dahshan, E. S. M. El-Horbaty, and A. B. M. Salem, "Classification using deep learning neural networks for brain tumors," *Future Computing and Informatics Journal*, vol. 3, no. 1, pp. 68-71, 2018.

[74] M. Shorfuzzaman, M. Masud, H. Alhumyani, D. Anand, and A. Singh, "Artificial neural network-based deep learning model for COVID-19 patient detection using X-ray chest images," *Journal of Healthcare Engineering*, vol. 2021, pp. 1-16, 2021.

[75] T. Hoefler, D. Alistarh, T. Ben-Nun, N. Dryden, and A. Peste, "Sparsity in deep learning: Pruning and growth for efficient inference and training in neural networks," *The Journal of Machine Learning Research*, vol. 22, no. 1, pp. 10882-11005, 2021.

[76] B. Li and Y. He, "An improved ResNet based on the adjustable shortcut connections," *IEEE Access*, vol. 6, pp. 18967-18974, 2018.

[77] J. Duan, T. Shi, H. Zhou, J. Xuan, and S. Wang, "A novel ResNet-based model structure and its applications in machine health monitoring," *Journal of Vibration and Control*, vol. 27, no. 9-10, pp. 1036-1050, 2021.

[78] G. N. Nguyen, N. H. Le Viet, M. Elhoseny, K. Shankar, B. B. Gupta, and A. A. Abd El-Latif, "Secure blockchain enabled Cyber–physical systems in healthcare using deep belief network with ResNet model," *Journal of parallel and distributed computing*, vol. 153, pp. 150-160, 2021.

[79] S. Ayyachamy, V. Alex, M. Khened, and G. Krishnamurthi, "Medical image retrieval using Resnet-18," *Medical Imaging 2019: Imaging Informatics for Healthcare, Research, and Applications*, vol. 10954, pp. 233-241, SPIE, 2019.

[80] M. Gao, D. Qi, H. Mu, and J. Chen, "A transfer residual neural network based on ResNet-34 for detection of wood knot defects," *Forests*, vol. 12, no. 2, p. 212, 2021.

[81] L. Wen, X. Li, and L. Gao, "A transfer convolutional neural network for fault diagnosis based on ResNet-50," *Neural Computing and Applications*, vol. 32, pp. 6111-6124, 2020.

[82] B. Yu, L. Yang, and F. Chen, "Semantic segmentation for high spatial resolution remote sensing images based on convolution neural network and pyramid pooling module," *IEEE Journal of Selected Topics in Applied Earth Observations and Remote Sensing*, vol. 11, no. 9, pp. 3252-3261, Sep. 2018.

[83] E. S. Ghith and F. A. A. Tolba, "Design and optimization of PID controller using various algorithms for micro-robotics system," *Journal of Robotics and Control (JRC)*, vol. 3, no. 3, pp. 244-256, 2022.

[84] A. K. Hado, B. S. Bashar, M. M. A. Zahra, R. Alayi, Y. Ebazadeh, and I. Suwarno, "Investigating and optimizing the operation of microgrids with intelligent algorithms," *Journal of Robotics and Control (JRC)*, vol. 3, no. 3, pp. 279-288, 2022.

[85] E. H. Kadhim and A. T. Abdulsadda, "Mini drone linear and nonlinear controller system design and analyzing," *Journal of Robotics and Control (JRC)*, vol. 3, no. 2, pp. 212-218, 2022.

[86] A. Ma'arif and A. Çakan, "Simulation and arduino hardware implementation of dc motor control using sliding mode controller," *Journal of Robotics and Control (JRC)*, vol. 2, no. 6, pp. 582

[87] A. Ma'arif and N. R. Setiawan, "Control of DC motor using integral state feedback and comparison with PID: simulation and Arduino implementation," *Journal of Robotics and Control (JRC)*, vol. 2, no. 5, pp. 456-461, 2021.

[88] H. Maghfiroh, A. Ramelan, and F. Adriyanto, "Fuzzy-PID in BLDC motor speed control using MATLAB/Simulink," *Journal of Robotics and Control (JRC)*, vol. 3, no. 1, pp. 8-13, 2022.

[89] M. Samuel, M. Mohamad, M. Hussein, and S. M. Saad, "Lane keeping maneuvers using proportional integral derivative (PID) and model predictive control (MPC)," *Journal of Robotics and Control (JRC)*, vol. 2, no. 2, pp. 78-82, 2021.

[90] A. Wajiansyah, S. Supriadi, A. F. O. Gaffar, and A. B. W. Putra, "Modeling of 2-DOF hexapod leg using analytical method," *Journal of Robotics and Control (JRC)*, vol. 2, no. 5, pp. 435-440, 2021.

[91] A. Surriani, M. Arrofiq, and F. Fahmizal, "Pemodelan Forward Kinematic dan Inverse Kinematic Robot Berlengan PUMA 560," *Jurnal Ilmiah Teknik Elektro Komputer Dan Informatika*, vol. 4, no. 2, pp. 66-75, 2019.

[92] P. Sutyasadi, "Control Improvement of Low-Cost Cast Aluminium Robotic Arm Using Arduino Based Computed Torque Control," *Jurnal Ilmiah Teknik Elektro Komputer Dan Informatika*, vol. 8, no. 4, pp. 650-659, 2022.

[93] P. Chotikunnan and Y. Pititheeraphab, "Adaptive P Control and Adaptive Fuzzy Logic Controller with Expert System Implementation for Robotic Manipulator Application," *Journal of Robotics and Control (JRC)*, vol. 4, no. 2, pp. 217-226, 2023.

[94] P. Chotikunnan, R. Chotikunnan, A. Nirapai, A. Wongkamhang, P. Imura, and M. Sangworasil, "Optimizing Membership Function Tuning for Fuzzy Control of Robotic Manipulators Using PID-Driven Data Techniques," *Journal of Robotics and Control (JRC)*, vol. 4, no. 2, 2023.

[95] P. Chotikunnan and R. Chotikunnan, "Dual design PID controller for robotic manipulator application," *Journal of Robotics and Control (JRC)*, vol. 4, no. 1, pp. 23-34, 2023.

[96] P. Chotikunnan, B. Panomruttanarug, and P. Manoonpong, "Dual Design Iterative Learning Controller for Robotic Manipulator Application," *Control Engineering and Applied Informatics*, vol. 24, no. 3, pp. 76-85, 2022.

[97] P. Chotikunnan and B. Panomruttanarug, "Practical design of a time-varying iterative learning control law using fuzzy logic," *Journal of Intelligent & Fuzzy Systems*, vol. 43, no. 3, pp. 2419-2434, Jul. 2022.

[98] N. Widodo and A. Pamungkas, "Machine Vision-based Obstacle Avoidance for Mobile Robot," *Jurnal Ilmiah Teknik Elektro Komputer Dan Informatika*, vol. 5, no. 2, pp. 77-84, 2019.

[99] L. Amifia, M. Riansyah, and P. Putra, "Design of Logistic Transporter Robot System," *Jurnal Ilmiah Teknik Elektro Komputer Dan Informatika*, vol. 6, no. 1, pp. 19-28, 2020.

[100] P. Rosyady and R. Sumiharto, "Highway Visual Tracking System using Thresholding and Hough Transform," *Jurnal Ilmiah Teknik Elektro Komputer Dan Informatika*, vol. 4, no. 2, pp. 93-99, 2019, doi: 10.26555/jiteki.v4i2.12016.

[101] R. Muwardi, M. Yunita, H. Ghifarsyam, and H. Juliyanto, "Optimize Image Processing Algorithm on ARM Cortex-A72 and A53," *Jurnal Ilmiah Teknik Elektro Komputer Dan Informatika*, vol. 8, no. 3, pp. 399-409, 2022, doi: 10.26555/jiteki.v8i3.24457.

[102] D. Sharma and N. Agrawal, "Development of Modified CNN Algorithm for Agriculture Product: A Research Review," *Jurnal Ilmiah Teknik Elektro Komputer Dan Informatika*, vol. 8, no. 1, pp. 167-174, 2022, doi: 10.26555/jiteki.v8i1.23722.

[103] R. Bello and C. Oluigbo, "Deep Learning-Based SOLO Architecture for Re-Identification of Single Persons by Locations," *Jurnal Ilmiah Teknik Elektro Komputer Dan Informatika*, vol. 8, no. 4, pp. 599-609, 2022, doi: 10.26555/jiteki.v8i4.25059.

[104] B. Suprapto, A. Wahyudin, H. Hikmarika, and S. Dwijayanti, "The Detection System of Helipad for Unmanned Aerial Vehicle Landing Using YOLO Algorithm," *Jurnal Ilmiah Teknik Elektro Komputer Dan Informatika*, vol. 7, no. 2, pp. 193-206, 2021, doi: 10.26555/jiteki.v7i2.20684.

[105] R. Bello, C. Oluigbo, and O. Moradeyo, "Motorcycling-Net: A Segmentation Approach for Detecting Motorcycling Near Misses," *Jurnal Ilmiah Teknik Elektro Komputer Dan Informatika*, vol. 9, no. 1, pp. 96-106, 2023, doi: 10.26555/jiteki.v9i1.25614.